Dynamic Effective Stress Analysis of a Centerline Tailings Dam – Case Study

Paola Torres
Knight Piésold Consultores S.A., Lima, Lima, Peru

Jorge Macedo
Georgia Institute of Technology, Atlanta, Georgia, United States

Solange Paihua
Knight Piésold Consultores S.A., Lima, Lima, Peru

ABSTRACT: This study presents the results for the dynamic effective stress analysis performed to evaluate the seismic performance of a center-line tailings dam in the South American Andes. To characterize the seismic demand at the project site, a probabilistic seismic hazard analysis (PSHA) was performed, producing deterministic-based and probabilistic-based seismic design criteria. The PSHA study shows that the project site is affected by both subduction interface and subduction intraslab ground motions. In addition, the PSHA study produced spectrally matched ground motions for the subsequent dynamic analyses. This paper presents the 2D dynamic analysis of a tailings dam subjected to the maximum credible earthquake (MCE). The centerline tailings dam is planned to be raised up to 90-m high, and it will be composed by a starter dam and successive raisings. The dynamic analyses were performed with the software FLAC, using the UBCHYST constitutive model for materials that are not expected to produce large excess pore pressures, and the PM4Silt model for the materials that may generate excess pore pressures due to cyclic loading. The results suggest that there are no failure mechanisms by the end of the ground motions during the numerical simulations; however, there are considerable displacements. The results help to plan the overall operational management of the tailings facility.

1 INTRODUCTION

This paper presents the dynamic effective stress analysis of a centerline tailings dam, located in the South American Andes. The centerline construction method has been selected to build the dam that is part of the tailings storage facility (TSF) because it allows optimization of available storage while minimizing the volume of dam material. The dam will retain tailings during the operation, and also after closure. It will have a height of 90 m, and its crest length will be approximately 56 0m. The dam will be built in six stages, which consider a starter dam and five sequential center-lined raisings supported by an upstream rockfill platform. Downstream slopes are equal to 2H:1.0V and 2.3H:1.0V for the starter dam and raisings, respectively, whereas the upstream slopes are 1.7H:1.0V and 1.5H:1.0V.

The analyses performed in this study were conducted to evaluate the seismic performance of the dam, which is controlled by the earthquake-induced permanent deformations and the intactness of the seepage control system. There are a number of simplified procedures to perform initial evaluations of the overall seismic performance of a dam (e.g. Bray & Macedo, 2019; Bray et al., 2018). However, when liquefiable materials are present in the dam body or its foundation, more rigorous procedures should be employed, which was the strategy considered in this study.

This paper presents the results of fully coupled stress-flow dynamic analyses using design ground motions provided by a probabilistic seismic hazard study (PSHA) for the dam area. We have captured the tailings behavior observed in cyclic laboratory tests by using the constitutive

model PM4Silt (Boulanger & Ziotopoulou, 2018). The nonlinear behavior of non-liquefiable materials was accounted for by employing the model UBCHYST (Naesgaard, 2011). These user-defined constitutive models are incorporated into the commercially available computer code FLAC 8.0 (Itasca, 2016).

2 DESCRIPTION OF THE DAM, FOUNDATION, AND TAILINGS MATERIALS

The information collected from geotechnical site investigations was reviewed and interpreted to characterize the dam, foundation, and tailings materials. The dam considered in this study has not been built yet; hence, some material properties have been estimated based on laboratory tests performed on samples obtained from quarries and tailings samples obtained from a pilot process plant. Foundation properties were estimated based on field tests (e.g., permeability and geophysical tests) when this information was available.

2.1 *Dam*

The dam is mainly composed of structural fill, in addition to the core, filter/drain, and rockfill materials, which are also present. The structural fill and core consist of moraine material (gravelly clay, GC); the core materials have a plasticity index (PI) of 15. The filter/drain is composed of coarse and medium sand, while the rockfill platform material is mainly composed of cobbles and boulders. The starter dam also includes an upstream geomembrane to prevent contact water from getting into the dam body. The soil particle-size fraction distribution of these materials is shown in Table 1, and Figure 1 presents the maximum cross-section of the dam, which has been considered in this study.

Table 1. Soil particle-size fraction distribution of the dam construction materials

Classification of soils	Structural fill [%]	Core [%]	Filter/drain [%]	Rockfill platform [%]
Cobbles and boulders	0 – 20	0 – 5	0	10 – 75
Gravel	30 – 50	15 – 40	0 – 35	25 – 45
Sand	20 – 40	30 – 40	65 – 95	0 – 40
Fines content*	10 – 30	25 – 45	0 – 5	0 – 5
Max. Particle Size	6"	4"	1"	6"
Plasticity Index	8 – 15	> 15	Non-plastic	Non-plastic

*Fines content defined as percent passing 0.075 mm (N°.200 sieve)

2.2 *Foundation*

The foundation is composed of two groups of rocks that belong to the Ambo and Copacabana geological groups, respectively. The Ambo group is mainly composed of a large proportion of quartz sandstone with thin horizons of siltstone and bituminous shales. The rock is moderately weathered, has a low to medium strength, and is slight to moderately fractured. The Copacabana group is mainly composed by limestone rocks with intercalations of dolomite horizons, calcareous breccia, calcareous sandstone, and siltstone. The upper stratum of this group is moderate to highly weathered, has a low strength, and is moderate to very fractured, while the lower stratum is slight to moderately weathered, has a medium to high strength, and is slight to moderately fractured.

2.3 *Tailings*

In the first year of operation, the TSF will receive tailings from the new process plant; after the second year, it will store tailings from an additional process plant, increasing the volume of tailings that need to be stored. Therefore, two types of tailings, denominated as tailings R and C, were characterized as part of this study. Tailings R classifies as silty clays (CL), have low to medium plasticity (PI = 9), 98% fines content, and an average specific gravity of 2.8. Tailings C classify mainly as sandy silts (ML), with an average fines content of 65%. They have null to low plasticity (PI = 4) and an average specific gravity of 2.81.

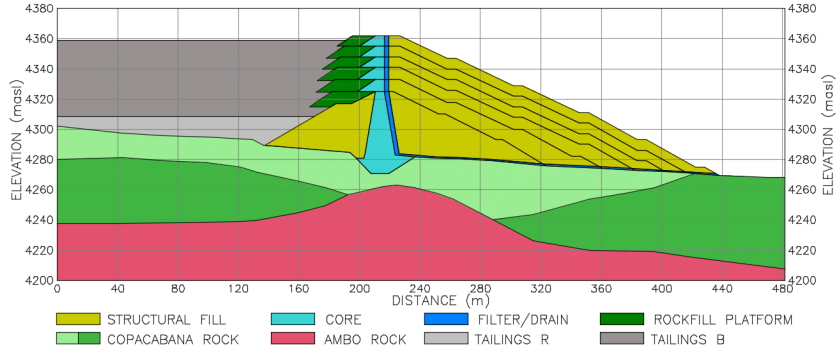

Figure 1. Maximum cross-section of the dam

3 SEISMIC DESIGN CRITERIA

Using the Canadian Dam Association (CDA) dam safety guidelines, the seismic risk associated with the dam was classified as "Extreme". For extreme hazard dams, CDA (2013) recommends the MCE or 10,000-year earthquake. The MCE was ultimately selected as the appropriate design earthquake for the dam. The resulting peak horizontal ground accelerations (PGA) for the MCE is 0.34g based on the 84th percentile of the deterministic acceleration spectrum, and it is associated with a Magnitude 8.0 Intraslab earthquake at a distance of 120 km from the project site.

Three acceleration design time-histories, provided by the PSHA study, have been used for the analyses. These time histories correspond to spectrally matched records that used recorded ground motions from the following earthquakes: (1) Lima, 1974; (2) Moquegua, 2001; and (3) Pisco, 2007. The ground motions used for the dynamic analyses are presented in Figure 2, and were applied to a quiet-boundary base of the numerical model as stresses.

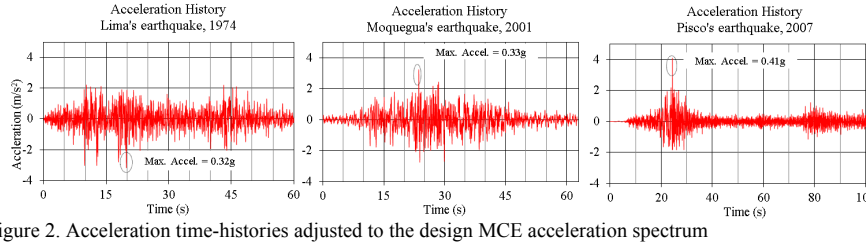

Figure 2. Acceleration time-histories adjusted to the design MCE acceleration spectrum

4 NUMERICAL MODEL

The dam was modeled using FLAC, which allows users to solve stress-strain geotechnical problems considering a fully explicit time-marching numerical formulation. The dimensions of the model and zones satisfy seismic wave transmission requirements according to Kuhlemeyer & Lysmer (1973) recommendations, which state that maximum zone dimension should be less than one-tenth of the maximum shear wavelength for a given material. The thickness of the zones in the FLAC model were 1 m. Figure 3 presents the FLAC dam model.

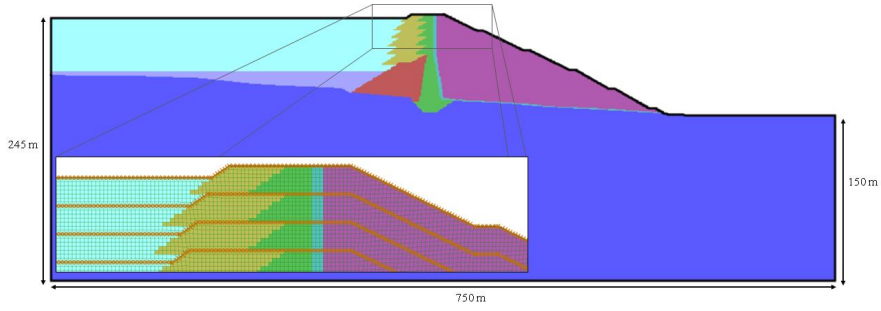

Figure 3. FLAC model for the dam evaluated in this study

5 STATIC ANALYSIS

Before performing the dynamic analyses, the dam body and its foundation have been analyzed under gravity loads with drained conditions to establish the pre-earthquake stress state. We used the Mohr-Coulomb model for tailings and dam materials, and an elastic model for the bedrock. Bedrock elastic parameters were obtained from the multichannel analyses of surface waves (MASW), while for the dam materials, the properties were estimated based on shear wave velocity (Vs) measured on similar materials in the dam area. Along with the static analysis, flow analyses were performed to establish the pre-earthquake pore pressure distribution, i.e., the steady-state flow condition. Groundwater boundary conditions were applied to the model to obtain a water table descending through the filter/drain chimney and to assure the saturated condition of tailings. This represents a critical stability condition for the TSF, which was considered appropriate for the analyses. Table 2 presents the properties considered for the static and flow analyses, and Figure 4 presents the model's initial stress state.

Table 2. Material properties for static and flow analysis

Material	**Dry unit weight** γ_{dry} **(kN/m^3)**	**Friction angle** ϕ' **(º)**	**Cohesion** **c** **(kP)**	**Poisson ratio** **ν**	**Shear stiffness** **G*** **(MPa)**	**Bulk Modulus** **K**** **(MPa)**	**Porosity** **n**	**Hydraulic conductivity** **k** **(m/s)**
Structural fill	21.0	38	0	0.35	70	210	0.30	1E-07
Core	20.0	34	8	0.35	67	200	0.35	1E-07
Filter/drain	17.0	35	0	0.33	46	120	0.33	2E-03
Rockfill platform	20.5	40	0	0.30	78	169	0.26	1E-03
Tailings	14.5	30	0	0.35	3.5	10.5	0.48	1E-07
Bedrock	25.0	-	-	0.28	382	740	0.15	1E-06

*Static shear stiffness (G) was taken as $0.1G_{max}$. G_{max} is the small strain shear modulus estimated as $G_{max}=\rho V_s^2$, where ρ is the total density of the material.
**Bulk modulus (K) is calculated as K=G*2*(1+ ν)/(3*(1-2 ν)).

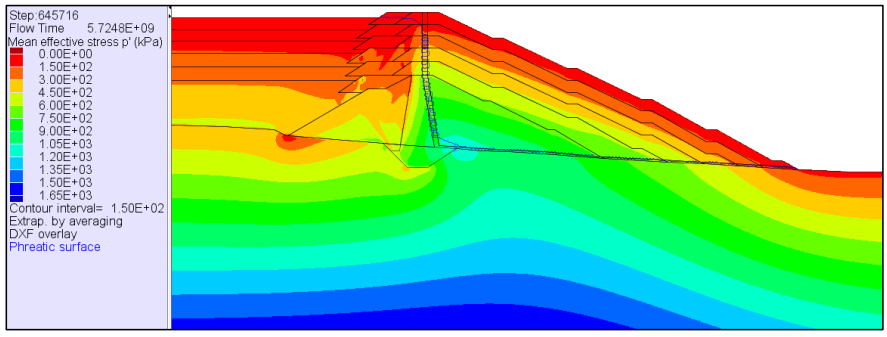

Figure 4. Pre-earthquake mean effective stress (p') and water table location

6 DYNAMIC ANALYSIS

6.1 *Constitutive models*

The UBCHYST constitutive model was selected for the structural fill, core, filter/drain, and rockfill platform materials. These materials have been considered non-liquefiable due to their high permeability, particle size, or compaction degree. The non-linear hysteretic UBCHYST model is a robust, relatively simple, total stress model. UBCHYST was developed at the University of British Columbia for dynamic analyses of soil subjected to earthquake loading. Typically, the model is used for fine-grained soils (silts and clays) with undrained strength parameters, for free-draining granular soil with drained strength parameters or in non-saturated granular soils. Its characteristics include the reduction of the shear secant modulus with strain, emulation of marching or ratcheting to occur when there is a static shear bias, and the option of allowing a permanent modulus reduction as a function of maximum past shear stress ratio (Naesgaard 2011).

The PM4Silt constitutive model was selected to represent the response of tailing materials because they are expected to be susceptible to liquefaction. Tailings have not been deposited at the TSF yet, so there is no field available data from the likes of cone penetration tests (CPTs). Nevertheless, due to tailings nature is inferred that tailings would develop excess pore water pressures and/or likely undergo liquefaction due to earthquake shaking. The PM4Silt plasticity model was developed and implemented by Boulanger & Ziotopoulou (2018) for representing low-plasticity silts and clays in geotechnical earthquake engineering applications. The model is focused on approximating a range of undrained monotonic and cyclic loading responses of saturated low-plasticity silts and clays that exhibit stress-history normalized behaviors, as opposed to the responses of purely nonplastic silts and sands (Boulanger & Ziotopoulou, 2018).

6.2 *Non-liquefiable materials input parameters*

That small strain (dynamic) shear stiffness, G_{max}, for bedrock was estimated from the shear wave velocity measurements. The Bedrock was modeled as an elastic material with a shear wave velocity of 1200 m/s. In the case of the filter/drain, structural fill, and rockfill platform, G_{max} was estimated using shear wave velocity measurements in similar material from existing dams. Furthermore, G_{max} of the core material was estimated based on resonant column test results. The G_{max} values for different materials were applied to the model with an effective confinement stress dependency according to Equation 1, proposed by Seed et al. (1970, 1984),

$$G_{max} = 21.7 k_{2,max} Pa \left(\frac{\sigma'_m}{Pa}\right)^{0.5} \quad (1)$$

where G_{max}, $k_{2,max}$, P_a and σ'_m are the small strain shear modulus, modulus coefficient, atmospheric pressure, and the mean confining pressure, respectively. Equation 1 makes G_{max} and bulk modulus values vary with depth across the height of the dam.

Table 3. Dam and foundation properties for dynamic analysis

Material	Model	Dry unit weight γ_{dry} (kN/m^3)	Modulus coefficient $k_{2,máx}$	Poisson ratio N	Small strain shear modulus G_{max} @1atm (MPa)	Bulk modulus K_{max} @1atm (MPa)
Structural fill	UBCHYST	21.0	160	0.35	350	1049
Core	UBCHYST	20.0	140	0.35	308	924
Filter/drain	UBCHYST	17.0	110	0.33	242	631
Rockfill platform	UBCHYST	20.5	180	0.30	396	858
Bedrock	Elastic	25.0	-	0.28	3817	7402

The summary of the dam and foundation dynamic properties is presented in Table 3 and it shows the $k_{2,máx}$ values selected for construction materials which are in the range expected for gravels according to Seed et al. (1984).

The shear modulus and damping ratio curves used in the dynamic analyses were calibrated using several references. The curves from Rollins et al. (1998) were considered for rockfill materials, the curves from Darendeli (2001) were considered for the structural fill and filter/drain material, and the Seed & Idriss (1970, 1986) curves for sands and gravels were also considered. Shear modulus reduction and damping ratio curves for the core material were obtained from resonant column (RC) tests and were also considered for the structural fill due to its similarity. All these experimental-based and laboratory curves were used to calibrate the UBCHYST model. Figure 5 presents the cyclic FLAC simulations obtained for the dam materials.

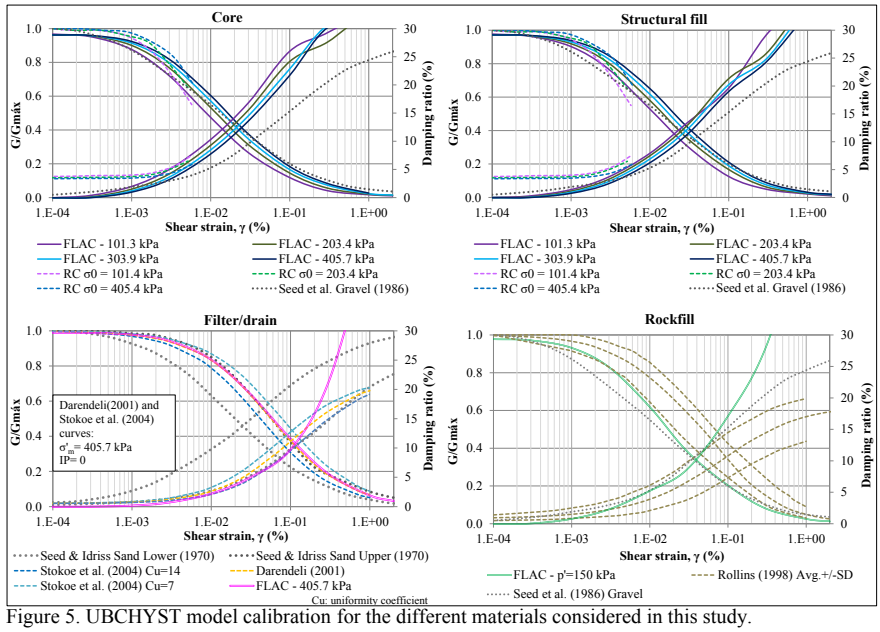

Figure 5. UBCHYST model calibration for the different materials considered in this study.

The strength parameters of the rockfill platform and structural fill were estimated based on data from Leps (1970). The parameters selected for the rockfill platform are between the lower-bound values and the average values for rockfill materials, whereas the parameters selected for the structural fill are comparable to the lower-bound values. The friction angle ϕ was estimated based on Barton & Kjaersnli (1981), using Equation 2:

$$\phi = \phi_1 - \Delta\phi log(\frac{\sigma'_3}{Pa}) \quad (2)$$

where, σ'_3, ϕ_1, and $\Delta\phi$ are minor principal effective stress, reference friction angle (at σ'_m = Pa), and friction angle reduction for every log cycle of stress level increase, respectively.

The summary of the strength parameters and UBCHYST calibration parameters for the dam materials are presented in Table 4. These are the final values used in FLAC simulations curves shown in Figure 5. Calibration parameters for core and structural fill were obtained for specific stress ranges by using results of resonant column test.

Table 4. Strength parameters and UBChyst calibration parameters

Material	Friction angle			Cohesion	Mean effective stress range	UBCHYST calibration parameters				
	ϕ (°)	ϕ_1 (°)	Δϕ (°)	c (kPa)	σ'_m (kPa)	Hn	Hrf	Hrm	Hdfac	Hdmof1
Structural fill	LEPS	40	6	0	0-150 150-250 250-350 350-450 >450	2.0 2.5 2.7 2.7 2.7	0.98	1	0.7	1
Core	34	-	-	8	0-150 150-250 250-350 350-450 >450	3.0 3.5 3.7 3.7 3.7	0.98	1	0.7	1
Filter/drain	35	-	-	0	0	1	0.98	1	0.6	1
Rockfill platform	LEPS	45	6	0	0	2	0.7	1	0.8	1

6.3 *Liquefiable materials (tailings) input parameters*

As previously discussed, the PM4Silt constitutive model was used to model the response of tailings materials. To characterize the tailings cyclic behavior and to calibrate the PM4Silt constitutive model several laboratory tests were conducted: cyclic simple shear (CSS), consolidated undrained, and drained triaxial shear (CUTX and CDTX), monotonic simple shear (DSS) and bender element test.

As commonly observed for tailings, the slope of the liquefaction resistance curves (i.e. cyclic stress ration or CRS versus number of cycles for liquefaction) defined by multiple CSS tests for both types of tailings are quite flat. All cyclic resistance ratio (CSR) values are modest; they do not exceed a value of 0.2. It was also observed that raising the consolidation stress level from 100 kPa to 300 kPa or 400 kPa did not produce the expected reduction in normalized cyclic resistance, often characterized by a Kσ factor less than 1, but in fact, appeared to slightly raise the resistance. This resistance may be related to the compressible nature of the fine tailings, as there is a general trend for the densities to be higher for higher stress specimens.

The primary input parameters of the PM4Silt constitutive model are the undrained shear strength ratio ($S_{u,cs}/\sigma'_{vc}$) (or undrained shear strength $S_{u,cs}$), the shear modulus coefficient (G_o), the contraction rate parameter (h_{po}), and an optional post-strongshaking shear strength reduction factor. The secondary input parameters of the model have default values, but they can be set according to the available information for the material being evaluated.

$S_{u,cs/\sigma'vc}$ value was estimated from DSS tests, as well as the secondary parameter bounding surface parameter ($n_{b,wet}$). The parameter $n_{b,wet}$ was set to 1.0 because this limits the peak shear resistance to $S_{u,cs,eq}$ in the simulation, which matches the strain-hardening response observed in the DSS test. Moreover, G_o and shear modulus exponent (n_G) values were calculated from the bender element test results. Finally, secondary parameters φ_{cv} y λ were obtained from the critical state line (CLS). CLS for tailings R and B were generated from CU and CD triaxial data.

Based on previously defined parameters, undrained cyclic loading with uniform CSR was simulated on FLAC to find the value of h_{po} that would best adjust the fit to the experimentally observed liquefaction resistance curves. We also examined the stress-strain and stress-path responses in the experiments and the numerical simulations to modify secondary parameters in the model. The secondary parameters were modified to flatten the liquefaction resistance curve and to generate stress-strain and excess pore-pressure responses similar to those experimentally observed. The summary of the input parameters for the PM4Silt model are presented in Table 5. Figure 6 shows the experimental-based and numerical-based liquefaction resistance curves.

Table 5. Input parameters for PM4Silt calibrations for tailings

Input parameters		**Default value**	**Calibration parameters**	
			Tailings R	**Talings B**
Primary parameters				
Undrained shear strength ratio at critical state	$S_{u,cs}/\sigma'_{vc}$	-	0,2	0,16
Shear modulus coefficient	G_o	-	413	451
Contraction rate parameter	h_{po}	-	14	6.5
Secondary parameters				
Initial void ratio	e_o	0.9	0.82	0.98, 0.86*
Shear modulus exponent	n_G	0.75	0.712	0.657
Critical state friction angule	φ_{cv}	32	35	36
Compressibility in e-ln(p') space	λ	0.06	0.063	0.0454
Sets bounding p_{min}	$r_{u,max}$	$p_{min}=p_{cs}/8$	Default	Default
Bounding surface parameter	$n^{b,wet}$	0.8	1	1
Bounding surface parameter	$n^{b,dry}$	0.5	Default	Default
Dilation surface parameter	n^d	0.3	Default	Default
Dilatancy parameter	A_{do}	0.8	0,6	Default
Plastic modulus ratio	h_o	0.5	Default	Default
Fabric term	Z_{max}	$10 \leq 40(S_u/\sigma'_{vc}) \leq 20$	80	65
Fabric growth parameter	c_z	100	75	Default
Strain accumulation rate factor	c_ξ	$0.5 \leq (1.2S_u/\sigma'_{vc} +0.2) \leq 1.3$	0.9	Default
Modulus degradation factor	C_{GD}	3	Default	Default
Plastic modulus factor	$C_{k\alpha f}$	4	Default	Default

*0.98 value was used for the ten superficial meters of tailings, for deeper tailings, the value 0.86 was assigned.

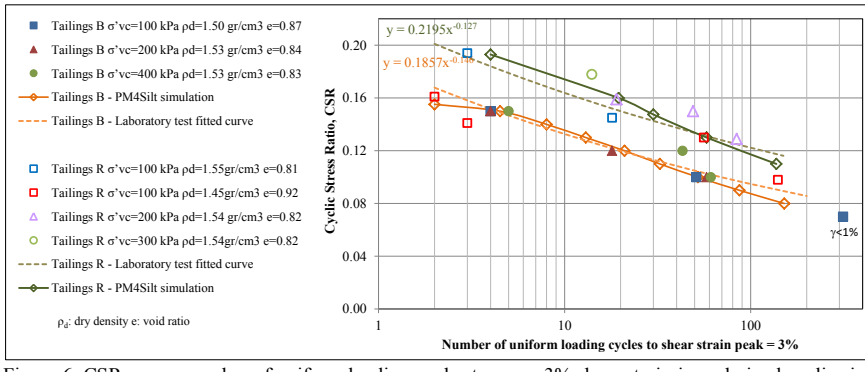

Figure 6. CSR versus number of uniform loading cycles to cause 3% shear strain in undrained cyclic simple shear tests – Curves for tailings B and R

7 RESULTS AND DISCUSSION

We discuss in this section the seismic response of the tailings-dam-foundation system, considering the design ground motion that led to the more conservative results. The FLAC model estimated maximum horizontal displacement at the dam crest of 2.75 m and 1 m towards the upstream and downstream direction, respectively, as shown in Figure 7. In addition, a maximum vertical deformation of 1.4 m was computed, as shown in Figure 8. The filter/drain and core experienced a range of horizontal displacements between 0.3 m to 1.0 m in the crest and up to 1.0 m of vertical displacement. These displacements are considered to be acceptable as it is not expected that they could affect the continuity of core materials, which have an original width of 3 m and 4 m, respectively.

Figures 7 77and 8 also show that the area with the highest displacements is the upstream part of the crest. Displacements at the dam crest are caused primarily by an upstream rotation of the top portion of the upstream rockfill platform into the liquefied tailings. It should be noted that the analyses considered that the pond in the tailings deposit is in contact with the upstream crest slope and that the tailings and core material are saturated. These conditions allowed the generation of pore pressures, which promoted the generation of shear strain deformations in specific areas inside the core. However, these shear strains did not extend towards the upstream or downstream direction during the analyses, so a failure mechanism was not apparent. An additional observation is that the horizontal and vertical displacements in the rockfill platforms caused by the design ground motions consistent with the MCE earthquake may temporarily damage the tailings pipeline system.

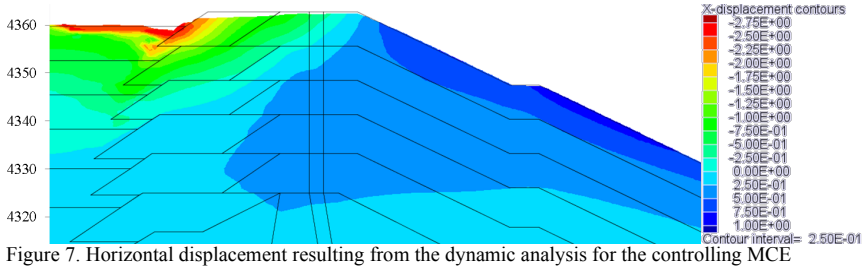

Figure 7. Horizontal displacement resulting from the dynamic analysis for the controlling MCE

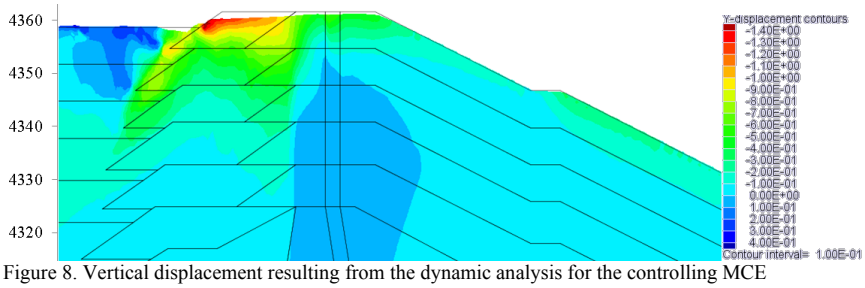

Figure 8. Vertical displacement resulting from the dynamic analysis for the controlling MCE

The seismic-induced excess pore water pressure ratio, Ru (u/σ'_{vo}), was monitored in all tailings zones of the model. During the analyses, zones where liquefaction has been triggered (pore pressure ratio Ru > 0.70 to 1.0) are tracked. These zones are shown in red color in Figure 9. It can be observed the almost 30 m to 40 m depth of tailings have liquefied.

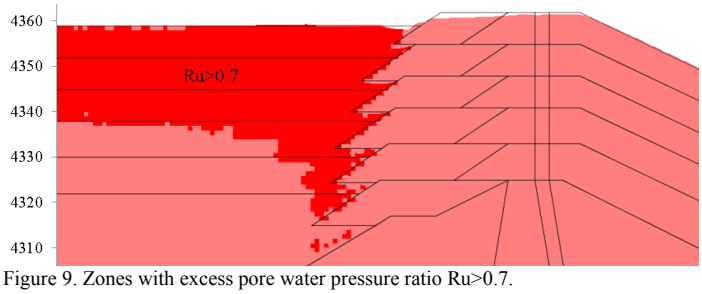

Figure 9. Zones with excess pore water pressure ratio Ru>0.7.

8 SUMMARY AND CONCLUSIONS

The results suggest that there are no clear failure mechanisms by the end of the numerical simulations considering the design ground motion used in this study. Furthermore, the numerical results suggest that the damage to the core and filter/drain would be minor to moderate and that the loss of freeboard may not compromise the dam function during the MCE. However, it is likely that reparations may be needed after an earthquake comparable with the MCE earthquake considered in this study.

The results also highlight the need to maintain a tailings beach in well-drained conditions - with the pond away from the crest dam - and also the importance of reinforcement with rockfill platforms. A tailings beach in well-drained conditions would limit the generation of pore pressures during a seismic event; likewise, the reinforcement with rockfill platforms is expected to contribute to the dam's seismic performance.

The results from this study are applicable only if the material properties during the dam rainings (e.g., dam properties and tailing properties) are consistent with the assumptions made in this study; hence, these properties should be evaluated during the operation. In addition, a larger set of dynamic analyses with a large set of ground motions should be performed to better characterize the dynamic response of the dam. Finally, the design ground motions considered in this study were based on ground-motion models (GMMs) that are expected to be updated in the near future (e.g, based on the. NGASub project outcomes). Hence, the design ground motions should be updated once updated GMMs are made available to the geotechnical earthquake engineering community.

9 REFERENCES

Barton, N. & Kjærnsli, B., 1981. Shear strength of rockfill. *J. of the Geotech. Eng. Div., Proc. of ASCE*, Volume 107:GT7: 873-891. Proc. Paper 16374, July.

Boulanger, R. W., & Ziotopoulou, K., 2018. PM4Silt (Version 1): a silt plasticity model for earthquake engineering applications. *Report No. UCD/CGM-18/01, Center for Geotechnical Modeling, Department of Civil and Environmental Engineering, University of California, Davis, CA, 108 pp.*

Bray, J. D., Macedo, J., & Travasarou, T., 2018. Simplified procedure for estimating seismic slope displacements for subduction zone earthquakes. *Journal of Geotechnical and Geoenvironmental Engineering*, *144*(3), 04017124.

Bray, J. D., & Macedo, J., 2019. Procedure for estimating shear-induced seismic slope displacement for Shallow Crustal Earthquakes. *Journal of Geotechnical and Geoenvironmental engineering*, *145*(12), 04019106.

Darendeli, M. B., 2001. Development of a new family of normalized modulus reduction and material damping curves [Ph. D. dissertation]. Austin: University of Texas.

Itasca 2016, FLAC 8.0 (Fast Lagrangian Analysis of Continua) User Manual, Itasca Consulting Group, Inc., Minneapolis

Kuhlemeyer, R. L., & Lysmer, J., 1973. Finite element method accuracy for wave propagation problems. *Journal of Soil Mechanics & Foundations Div*, *99*(Tech Rpt).

Leps, T.M. 1970. Review of Shearing Strength of Rockfill. American Society of Civil Engineers, *Journal of Soil Mechanics and Foundation Division*, Volume 96: 1159-1170.

Naesgaard, E. 2011. A hybrid effective stress-total stress procedure for analyzing embankments subjected to potential liquefaction and flow. Ph.D. thesis, Civil Engineering Department, The University of British Columbia, Vancouver, B.C.

Rollins, K. M., Evans, M. D., Diehl, N. B., & III, W. D. D., 1998. Shear modulus and damping relationships for gravels. *Journal of Geotechnical and Geoenvironmental Engineering*, *124*(5), 396-405.

Seed, H. B., Wong, R. T., Idriss, I. M., & Tokimatsu, K., 1984. Moduli and damping factors for dynamic analyses of cohesionless soils. Rep. No.EERC 84-14, Earthquake Engineering Research Center, Univ. of California, Berkeley, California.

Seed, H. B., Wong, R. T., Idriss, I. M., & Tokimatsu, K., 1986. Moduli and damping factors for dynamic analyses of cohesionless soils. *Journal of geotechnical engineering*, *112*(11), 1016-1032.

Stokoe, K. H., Darendeli, M. B., Gilbert, R. B., Menq, F. Y., & Choi, W. K., 2004. Development of a new family of normalized modulus reduction and material damping curves. In *International Workshop on Uncertainties in Nonlinear Soil Properties and their Impact on Modeling Dynamic Soil Response*.